

Self-Assembled Liver Organoids Recapitulate Hepatobiliary Organogenesis *In Vitro*

Dipen Vyas,^{1*} Pedro M. Baptista,^{2,3*} Matthew Brovold,¹ Emma Moran,¹ Brandon Gaston,¹ Chris Booth,¹ Michael Samuel,⁴ Anthony Atala,¹ and Shay Soker¹

Several three-dimensional cell culture systems are currently available to create liver organoids. In general, these systems display better physiologic and metabolic aspects of intact liver tissue compared with two-dimensional culture systems. However, none reliably mimic human liver development, including parallel formation of hepatocyte and cholangiocyte anatomical structures. Here, we show that human fetal liver progenitor cells self-assembled inside acellular liver extracellular matrix scaffolds to form three-dimensional liver organoids that recapitulated several aspects of hepatobiliary organogenesis and resulted in concomitant formation of progressively more differentiated hepatocytes and bile duct structures. The duct morphogenesis process was interrupted by inhibiting Notch signaling, in an attempt to create a liver developmental disease model with a similar phenotype to Alagille syndrome. **Conclusion:** In the current study, we created an *in vitro* model of human liver development and disease, physiology, and metabolism, supported by liver extracellular matrix substrate; we envision that it will be used in the future to study mechanisms of hepatic and biliary development and for disease modeling and drug screening. (HEPATOLOGY 2017; 00:000–000)

Until recently, most of the available liver cell culture models have been standard two-dimensional (2D; monolayer) systems. However, these models did not accurately mimic human liver tissue development and physiology. Improvements in cell culture techniques have enabled the creation of tissue models that better mimic human liver tissue and can advance our understanding of liver disease origin and progression and aid in the development of novel and improved treatments.⁽¹⁾ Currently, there are several models of hepatic microtissue available that display human-specific metabolism and physiologic responses,^(2–8) but none are accurately able to mimic facets of liver organogenesis. Hence, the lack of key

cell types and the limitations observed in the replication of organ development are now central milestones being addressed by scientists to make these organoids more complex and mature. Alternatives such as humanized animal liver models,^(9–11) which can reproduce some human-specific drug metabolism, pathogen–host interactions, and diseases *in vivo*, also cannot replicate human liver development⁽¹²⁾ and are restricted to phenomena occurring at a postnatal stage. Our prior research,⁽¹³⁾ using an intact lobe of an acellular liver extracellular matrix (ECM), perfused with human fetal liver progenitor cells (hFLPCs), showed organization of liver-like tissue with partially functional hepatocytes and biliary ductal structures. In the

AFP, alpha-fetoprotein; ALB, albumin; CK19, cytokeratin 19; CYP3A4/CYP3A7, cytochrome P450 3A4/3A7; 2D/3D, two-dimensional/three-dimensional; DAPT, N-[(3,5-difluorophenyl)acetyl]-L-alanyl-L-phenylglycine-1,1-dimethylethyl ester; ECM, extracellular matrix; EpCAM, epithelial cell adhesion molecule; hFLPC, human fetal liver progenitor cell; HNF, hepatocyte nuclear factor; HPLC, high-performance liquid chromatography; LDM, liver differentiation medium; SOX9, SRY (sex determining region Y)-box 9.

Received March 28, 2016; accepted August 16, 2017.

Additional Supporting Information may be found at onlinelibrary.wiley.com/doi/10.1002/hep.29483/supinfo.

Supported by Fundación ARAID, Marie Curie Actions–European Commission (H2020-MSCA-IF-2014-660554), and Instituto de Salud Carlos III (PI15/00563, all to P.M.B.), and by a grant from the National Cancer Institute (National Institute of Health R01CA180149 to A.A. and S.S.).

*These authors contributed equally to this work.

Copyright © 2017 by the American Association for the Study of Liver Diseases.

View this article online at wileyonlinelibrary.com.

DOI 10.1002/hep.29483

Potential conflict of interest: Nothing to report.

current study, we created human liver organoids that were self-assembled *in vitro* from hFLPCs seeded onto small, acellular, liver-specific ECM discs. These three-dimensional (3D) liver organoids demonstrated simultaneous human hepatobiliary organogenesis and partial metabolic and secretory functions of intact human liver tissue. Beyond the applications for human liver development research and modeling of liver congenital diseases, this system may be incorporated in high-throughput platforms for drug activity and toxicity screening.

Materials and Methods

Supplies and reagents were from the following sources: Abcam (Cambridge, UK); Advanced Bioscience Resources (Alameda, CA); American Bio (Natick, MA); Amresco (Solon, OH); BD Biosciences (Franklin Lakes, NJ); Bethyl Laboratories (Montgomery, TX); Bioassay Systems (Hayward, CA); Cell Sciences (Canton, MA); Cell Signaling Technology (Beverly, MA); Cole-Palmer (Vernon Hills, IL); Dako (Carpinteria, CA); Invitrogen (Carlsbad, CA); Johnson and Johnson (Arlington, TX); Leica Biosystems (Buffalo Grove, IL); Leica GmbH (Germany); Life Technologies (Carlsbad, CA); Marshall Bioresources (North Rose, NY); Miltenyi Biotec Inc. (Auburn, CA); Olympus (Tokyo, Japan); Peprotech (Rocky Hill, NJ); PhoenixSongs Biologicals (Branford, CT); Phenomenex Inc. (Torrance, CA); Qiagen (Germantown, MD); Roche Life Sciences (Indianapolis, IN); Santa Cruz Biotechnology (Dallas, TX); J.L. Shepherd and Associates, Inc. (San Fernando, CA); Sigma-Aldrich (St. Louis, MO); Sakura Finetek (Torrance, CA); Tree Star Inc. (Ashland, OR); Worthington Biochemical Corporation (Lakewood, NJ).

LIVER HARVESTING AND DECELLULARIZATION

Livers from 4-5-week-old ferrets (Marshall Bioresources) were used throughout the experiments for decellularization and disc preparation. A detailed description of ferret liver harvesting and decellularization has been published.⁽¹⁴⁾ Briefly, livers were harvested with intact vessels, and the portal vein was cannulated with 16-gauge cannulae (Cathlon Clear; Johnson & Johnson). Livers were then connected to a pump (Masterflex L/S peristaltic pump with Masterflex L/S easy load pump head and L/S 14-gauge tubing; Cole-Palmer) and perfused with 2 L of distilled water at the rate of 6 mL/min. Livers were then perfused with 4 L of detergent made up of 1% Triton-X 100 (Sigma-Aldrich) with 0.1% ammonium hydroxide (Sigma-Aldrich). Finally, livers were perfused with 8 L of distilled water to wash out the decellularization detergent.

ACELLULAR LIVER DISC PREPARATION

To obtain liver discs, decellularized livers were cut into small lobes, embedded in optimal cutting temperature compound in plastic molds (Sakura Finetek), and flash-frozen with liquid nitrogen. These cryopreserved liver lobes were mounted onto a cryotome (Leica CM1950) to obtain liver ECM discs. The cryotome temperature was set at around -8°C to -10°C to maintain the liver lobes at warmer temperatures, facilitating thick and intact sectioning of liver lobes. Sections were cut at 300 μm thickness. To generate a disc from the liver sections, an 8-mm-diameter biopsy punch was used, which was equipped with a plunger in order to place the discs in a 48-well plate. The 48-well plates

ARTICLE INFORMATION:

From the ¹Wake Forest Institute for Regenerative Medicine, Wake Forest Baptist Health, Winston-Salem, NC; ²Aragon Health Research Institute (IIS Aragon), Zaragoza, Spain; ³CIBERehd, Madrid, Spain; ⁴Mass Spectrometry Core Facility, Lipid Sciences Department, Wake Forest Baptist Health, Winston-Salem, NC.

ADDRESS CORRESPONDENCE AND REPRINT REQUESTS TO:

Shay Soker, Ph.D.
Wake Forest Institute for Regenerative Medicine
391 Technology Way
Winston-Salem, NC 27101
Tel: + 1-336-713-7295
E-mail: ssoker@wakehealth.edu
or

Pedro M. Baptista, Pharm.D., Ph.D.
Aragon Health Research Institute (IIS Aragon)
Avda San Juan Bosco, 13
50009 Zaragoza
Spain
E-mail: pmbaptista@iisaragon.es

were kept inside the cryotome until the required numbers of discs were obtained. The discs were then air-dried for up to 4-6 hours or until they were almost dry. This is a critical step in disc preparation to preserve the intactness of the discs. Following the drying step, the discs were washed carefully with multiple washes of phosphate-buffered saline and kept in phosphate-buffered saline at 4°C until ready for sterilization. The discs were sterilized by gamma irradiation at a dose of 1.5 Mrad (J.L. Shepherd and Associates).

ISOLATION OF hFLPCs

Human fetal livers were obtained from Advanced Bioscience Resources and were at developmental stages between 18 and 21 weeks of gestation. A detailed description of isolation of hFLPCs has been published.⁽¹⁴⁾ Briefly, nonhepatic tissue was removed by scalpels, and livers were enzymatically digested at 37°C by 6 mg/mL collagenase type IV (Worthington Biochemical Corporation) and 2,000 units of deoxyribonuclease (Roche Life Sciences). Following digestion, hematopoietic and nonparenchymal cells were separated from the parenchymal cell fraction by density gradient using Histopaque-1077 (Sigma-Aldrich; 10771). The lower fraction cell pellet was resuspended in Kubota's medium,⁽¹⁵⁾ plated onto collagen-IV-coated (5 µg/cm²; Sigma-Aldrich; C5533) and laminin-coated (1 µg/cm²; BD Biosciences; 354259) 15-cm culture plates, and incubated at 37°C. The cells were washed the next day to remove blood cells and maintained in Kubota's medium for up to 7 days.

hFLPC SEEDING ON ACELLULAR DISCS AND MATRIGEL

hFLPCs were harvested from culture plates using collagenase-IV and counted. Sterilized discs were incubated with Kubota medium for 30-45 minutes prior to cell seeding and then air-dried in a biosafety cabinet. hFLPCs (3×10^5 to 5×10^5 cells) were suspended in 10 µL volume in seeding medium for each disc. The cell suspension was slowly pipetted on top of each disc and incubated for about 1 hour at 37°C for attachment before putting in additional seeding medium. As a 2D control, the same numbers of hFLPCs were seeded on collagen-IV-coated and laminin-coated 48-well tissue culture plates. Matrigel (Corning; 3562354) control experiments used hFLPCs (1×10^5) suspended in 60 µL lactate dehydrogenase elevating virus-free Matrigel (5.5 µg/mL) and placed in a well of a 96-well plate,

allowed to become a gel at 37°C for 30 minutes, and then supplemented with seeding medium. The next day, the discs and cells in 2D and Matrigel were incubated with liver differentiation medium (LDM) made of advanced Roswell Park Memorial Institute (RPMI) medium—containing ascorbic acid (10 mg/L), dexamethasone (10^{-7} M), cAMP (2.45 mg/L), human prolactin (1 µg/L), human glucagon (1 mg/L), human epidermal growth factor (40 µg/L; R&D Systems), niacinamide (5 mM), tri-iodothyronine (0.67 µg/L), alpha-lipoic acid (0.105 mg/L), (D-Ala², D-Leu⁵)-enkephalin acetate (0.056 µg/L), hepatocyte growth factor (20 ng/mL; Peprotech), Free Fatty Acid Mix (76 µL/L), human growth hormone (3.33 µg/L), high-density lipoprotein (10 mg/L; Cell Sciences), and oncostatin M (10 µg/L; Peprotech). All factors were obtained from Sigma-Aldrich unless stated otherwise. The culture medium was changed every 24 hours, and the discs were cultured for up to 3 weeks before harvesting them after 1 week and 3 weeks for immunohistochemical and molecular analyses, respectively. In some experiments 10 nM *N*-[(3,5-difluorophenyl)acetyl]-L-alanyl-2-phenylglycine-1,1-dimethylethyl ester (DAPT) was added to the medium to inhibit Notch signaling.

ALBUMIN AND UREA ASSAYS

For hepatocyte functional analysis, culture medium was collected at 7, 14, and 21 days from cells growing on discs, Matrigel, and in 2D culture. For standard control, adult human hepatocytes were grown in collagen-I/Matrigel sandwich culture, and medium was collected after 48 hours. The medium was stored at -80°C until it was used for analysis. For analyzing albumin (ALB) synthesis, an enzyme-linked immunosorbent assay was performed using a human ALB ELISA kit (Bethyl Laboratories Inc.; E101). At least three different media samples were used and analyzed in triplicate. ALB concentrations were normalized per nanogram of DNA. Urea was measured by colorimetric assay using the Quantichrom Urea Assay Kit (Bioassay Systems; DIUR-500) and normalized per nanogram of DNA.

DRUG METABOLISM ASSAY

Liver organoids were incubated with phenobarbital (1 mM) for inducing cytochrome P450 (CYP450) enzymes for up to 48 hours prior to adding diazepam and 7-ethoxy coumarin for drug metabolism assay. The culture medium was collected at 3, 6, 12, and 24 hours after addition of diazepam and 7-ethoxy coumarin.

Trichloroacetic acid was added to medium at 1:4 volume, and the samples were incubated overnight at 4°C. The samples were then centrifuged, and the supernatant was collected and stored at -20°C for liquid chromatographic-mass spectrometric analysis. The metabolites were analyzed using high-performance liquid chromatography (HPLC)-tandem mass spectrometry. The auto-sampler and HPLC was a refrigerated Reliance Stacker and a dual-pump HPLC from Spark Holland. The triple-quadrupole mass spectrometer was a Quattro II with a Z-spray interface in the positive ion mode from MicroMass/Waters. The gradient used for column elution was based on the mix of the two following solvents:

HPLC solvent A=H₂O : methanol 95 : 5
with 0.15% formic acid

HPLC solvent B=methanol

The gradient of A:B was as follows: 0 minutes, 95:5; 10 minutes, 30:70; 20 minutes, 30:70; 22 minutes, 95:5; and 30 minutes, 95:5, with a flow rate of 200 µL/min. The source temperature was 80°C, and the desolvation temperature was 250°C using nitrogen. Cell medium (25 µL) was injected onto a Hypersil C18 BD 2.0 × 150 mm column (Phenomenex Inc.) at 50°C.

The multiple reaction monitoring pairs were as follows:

7-OH coumarin 339 > 163 *m/z*_{ce}=20 eV
Temazepam 301 > 255 *m/z*_{ce}=22 eV
Oxazepam 287 > 241 *m/z*_{ce}=22 eV
Diazepam 285 > 193 *m/z*_{ce}=30 eV
Nordiazepam 271 > 140 *m/z*_{ce}=30 eV
7-Ethoxycoumarin 191 > 163 *m/z*_{ce}=20 eV
4-OH coumarin 163 > 121 *m/z*_{ce}=24 eV
7-OH coumarin 163 > 107 *m/z*_{ce}=24 eV

Quantitation of the metabolites was performed using response curves in cell media from 10 pg/µL to 1000 pg/µL of each metabolite versus 500 pg/µL of internal standard 4-OH coumarin.

IMMUNOFLUORESCENCE ANALYSIS

The discs were fixed in 10% neutral-buffered formalin, tissue-processed, and paraffin-embedded for histological analysis. Using a microtome (Leica

Biosystems), 5-µm sections were cut from the embedded paraffin blocks and stained with hematoxylin and eosin using an Autostainer XL (Leica Biosystems). For immunofluorescence analysis, the slides were deparaffinized and the antibody target retrieval was carried out using Target Retrieval Solution (Dako; S1700). Following target retrieval, the slides were treated with 1% sodium borohydride in phosphate-buffered saline to reduce the tissue autofluorescence. The slides were then blocked for 30 minutes using serum-free protein block (Dako; X0909). Primary antibodies were diluted in antibody diluent (Dako; S0809) prior to adding to the slides. The slides were incubated overnight at 4°C with primary antibodies (Supporting Table S1). The next day, slides were washed (three times) with 1 × Tris-buffered saline with Tween 20 for 10 minutes. The slides were then incubated with appropriate Alexa Fluor secondary antibodies for 30 minutes and then washed three times with 1 × Tris-buffered saline with Tween 20. The slides were coverslipped with Prolong Gold Antifade Reagent with 4',6-diamidino-2-phenylindole (Cell Signaling Technology; 8961). Imaging was done using either a Leica DM4000B or an Olympus Fluoview FV10i.

GENE EXPRESSION STUDIES

DNA and RNA from the liver organoids were extracted using the Allprep DNA/RNA mini-kit (Qiagen). Complementary DNA was synthesized from 200-400 ng of total RNA using Superscript III first-strand synthesis (Life Technologies). RT-PCR was performed using the SuperScript III One-Step RT-PCR system with *Taq* DNA polymerase (Life Technologies). The primers used are listed in Supporting Table S2. Expression of genes analyzed was normalized using glyceraldehyde 3-phosphate dehydrogenase as a housekeeping gene. The PCR mix was run on a 1% agarose (American Bio) in a Tris acetate (Amresco) buffer. The bands were quantified by densitometric analysis using Image J software (n = 3-5). For cytochrome enzyme gene expression analysis, the organoids were not incubated with phenobarbital prior to the analysis. Quantitative real-time PCRs were carried out with Power SYBR Green PCR Master Mix (Life Technologies; 4367659) with a primer concentration of 300 nM and 5-10 ng of complementary DNA. Each reaction was split into three 10-µL technical replicates and put into a 384-well PCR plate. The conditions for the reactions were set at 95°C for 10 minutes, 40 cycles of 95°C for 15 seconds, and 60°C for 1 minute. Cycle

threshold values were determined by the ABI 7900HT Fast Real-Time PCR system and used for further data analysis. An unpaired *t* test was performed to determine the statistical significance of the samples.

FLOW CYTOMETRY

Following cell harvesting from culture dishes, a sample of cells was taken for fluorescence-activated cell sorting analysis. We performed this analysis on five different human fetal liver samples. Briefly, 200,000 cells were loaded per tube, fixed in 4% paraformaldehyde, and permeabilized with 0.1% saponin for intracellular markers. All cell samples were then pelleted and extensively blocked with the use of Fc blocking reagent (Miltenyi Biotec Inc.) for 15 minutes. Immunolabeling followed immediately with antibodies raised against epithelial cell adhesion molecule (EpCAM) phycoerythrin (EBA-1; Santa Cruz Biotechnology), intercellular adhesion molecule 1 allophycocyanin (HA58; BD Biosciences), alpha-fetoprotein (AFP; C-19; Santa Cruz Biotechnology) plus donkey anti-goat AF594 (Invitrogen), ALB fluorescein isothiocyanate (Bethyl Laboratories), cytokeratin 18 (CK18; Leica Biosystems GmbH) plus goat antimouse AF633 (Invitrogen), α -smooth muscle actin (ab5694; Abcam) plus donkey antirabbit AF488 (Invitrogen), CD105 phycoerythrin (266; BD Biosciences), and CD31 allophycocyanin (WM59; BD Biosciences) for 30 minutes in the dark at 4°C, followed by incubation with secondary antibody where needed for an additional 30 minutes after three washes. Negative controls were also prepared with mouse monoclonal anti-KLH immunoglobulin G1 isotype control antibodies fluorescein isothiocyanate, phycoerythrin, and allophycocyanin (340755, 340761, and 340754; BD Biosciences). In the case of the goat anti-AFP, mouse anti-CK18, and rabbit anti- α -smooth muscle actin antibodies, staining with secondary antibody alone was used as a negative control. Cell fluorescence was measured immediately after staining with a Becton Dickinson FACSCalibur flow cytometer (BD Biosciences), and all data were analyzed using FlowJo software, version 7.1.3 (Tree Star Inc.).

Results

LINEAGE SPECIFICATION OF HUMAN LIVER PROGENITORS INSIDE LIVER ECM

To create human liver organoids, we used our previously described decellularization method to fabricate

liver ECM scaffolds^(13,14,16,17) and then sectioned the scaffold and seeded sections (8-mm ECM discs) with hFLPC cultures that contained liver stromal (25%-40%) and endothelial (5%-15%) cells (Supporting Fig. S1). Within 2-3 weeks postseeding and culture in LDM, the cells and ECM self-assembled into 3D organoid structures with progressive cellular organization and differentiation (Supporting Fig. S2A-C). Large clusters of cells expressing hepatoblast markers (ALB⁺/CK19⁺/EpCAM⁺) were observed after 1 week, suggesting lineage restriction to the hepatoblast (Fig. 1A, top panel). After 3 weeks, there were clear changes in cell phenotype including ALB⁺/CK19⁻/EpCAM⁻ clusters and ALB⁻/CK19⁺/EpCAM⁺ ductal structures, suggesting parallel lineage specification into hepatocytes and polarized cholangiocytes, respectively (Fig. 1A, bottom panel). In contrast, hFLPCs seeded in Matrigel maintained their progenitor phenotype (ALB⁺/CK19⁺/EpCAM⁺) even after 3 weeks in culture, suggesting no parallel lineage specification into hepatocytes and cholangiocytes (Supporting Fig. S3A). We also identified asymmetrical primitive ductal structures with half of the circumference lined by CK19⁺ cells and the other by ALB⁺ cells, suggesting an intermediate phase of lineage specification⁽¹⁸⁾ (Fig. 1B). Progressive maturation of hFLPCs into hepatocytes was assessed by immunostaining, showing clusters of cells expressing both AFP and ALB after 1 week of culture, similar to fetal liver tissue (Fig. 1C, left panels). In contrast, after 3 weeks of culture, the hFLPCs completely lost AFP expression, which is suggestive of committed progenitors or a stage of adult liver cells (Fig. 1C, right panels). However, there were several nonstained cells, which constitute a mixed population of stromal cells (data not shown). Gene expression analysis showed expression of hepatocyte nuclear factor 4- α (HNF4 α), a hepatocyte differentiation regulator, in organoids after 3 weeks of culture, to levels that were higher than those of hFLPCs but lower than those detected in adult liver (Fig 1D). Cells in Matrigel showed higher levels of HNF4 α compared to hFLPCs, but the levels were lower compared to the organoids, suggesting less hepatocytic maturation in Matrigel (Supporting Fig. S3B). The differentiation results were further supported by expression of SRY (sex determining region Y)-box 9 (SOX9), a biliary marker (Supporting Fig. S3B). Similarly, expression of HNF6, a cholangiocyte differentiation regulator, progressively increased in organoids between 1 and 3 weeks of culture and was higher than in hFLPCs and adult liver tissue (Fig 1D). However, the expression

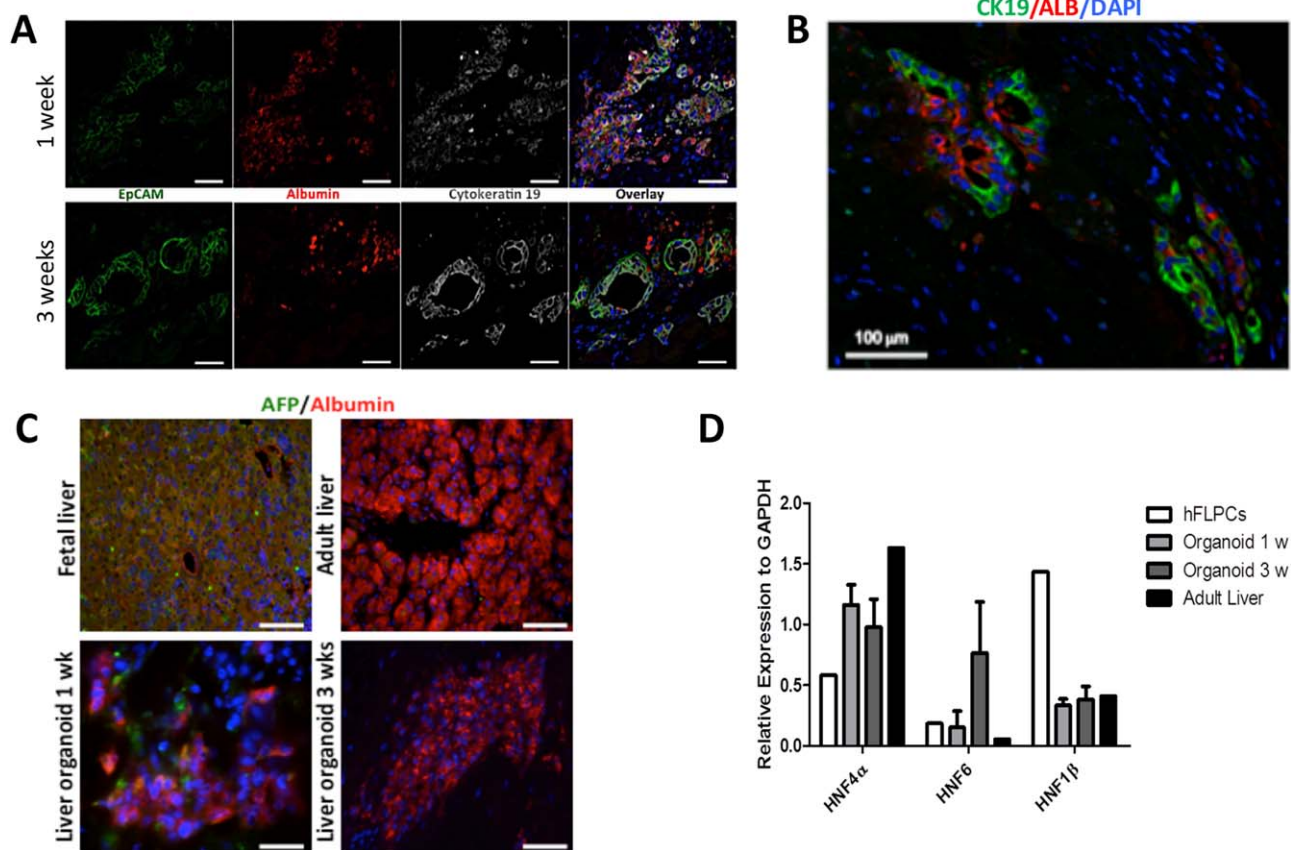


FIG. 1. Lineage specification of hFLPCs and formation of liver organoids. (A) Distribution and phenotypic characteristics of hFLPCs during 1 (top panel) and 3 (bottom panel) weeks of differentiation in culture. Cells were stained for EpCAM, ALB, and CK19 and for cell nuclei (4',6-diamidino-2-phenylindole). Scale bar, 20 μ m. (B) Immunostaining of liver organoids after 3 weeks of differentiation shows ductal structures containing cells expressing both CK19 (green) and ALB (red). (C) Expression of AFP (green) and ALB (red) in liver organoids after 1 and 3 weeks of differentiation in fetal and adult liver tissues. Scale bar, 20 μ m. (D) RT-PCR analysis of the expression of hepatic transcription factors HNF4 α , HNF6, and HNF1 β in freshly isolated hFLPCs, liver organoids after 1 and 3 weeks of differentiation, and adult liver tissue. Abbreviations: DAPI, 4',6-diamidino-2-phenylindole; GAPDH, glyceraldehyde 3-phosphate dehydrogenase.

level of HNF1 β , another regulator of cholangiocyte differentiation and bile duct formation, was higher in liver progenitors and showed similar lower expression after 1 and 3 weeks of culture, comparable to adult liver (Fig. 1D). Together, these results suggest premature hepatocytic and biliary phenotypes.

Liver tissue contains specific ECM molecules that surround the different liver zones and regulate specific cell differentiation, function, and regeneration.⁽¹⁹⁾ We observed normal patterning of ECM molecules around the bile duct structures and the hepatocyte clusters in the liver organoids (Supporting Figs. S2D and S12). Specifically, CK19⁺ bile ducts were surrounded by laminin and collagen-IV, which are involved in the

duct morphogenetic process, while ALB⁺ hepatocytes were surrounded by collagen-I and fibronectin.

HEPATOCTYTIC MATURATION OF HUMAN LIVER PROGENITOR CELLS

Immunohistological characterization of the hepatocyte clusters showed expression of several hepatocytic markers such as HNF4 α , α 1-antitrypsin, and cytochrome P450 3A4 (CYP3A4) after 3 weeks in culture (Fig. 2A). RT-PCR analysis confirmed the expression of mature hepatocyte markers including glucose 6-phosphatase, aspartate aminotransferase, and tyrosine aminotransferase

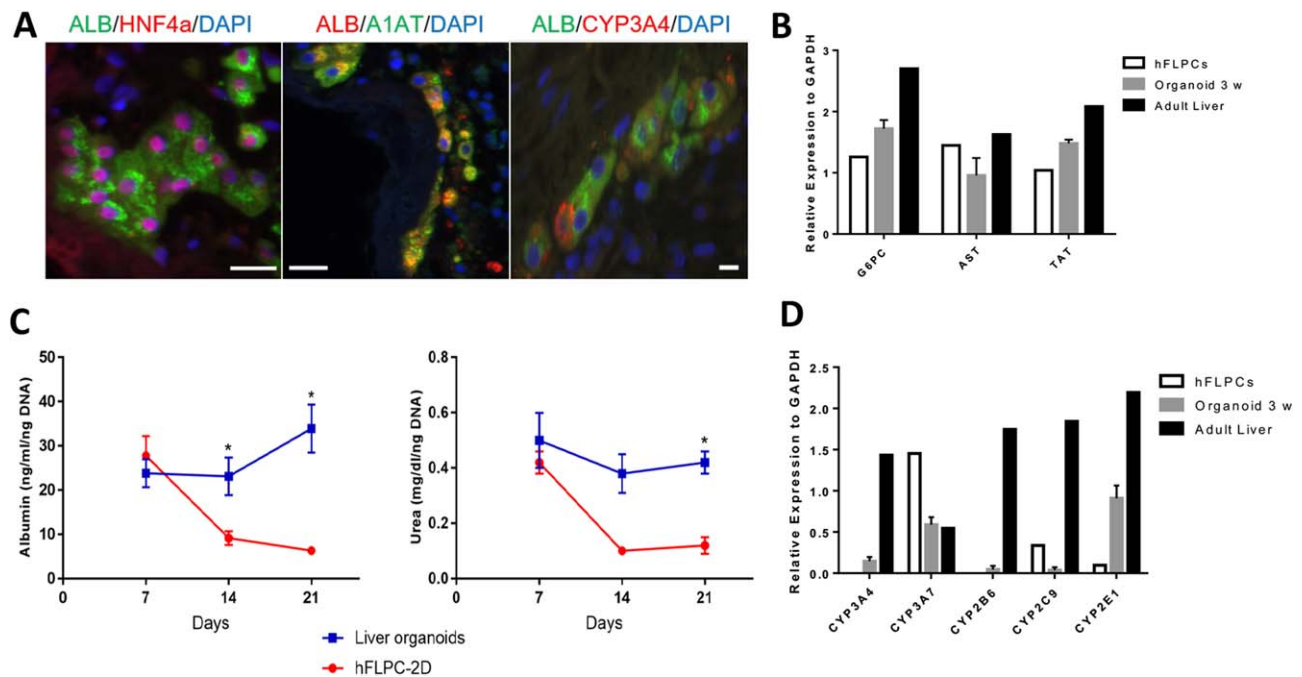


FIG. 2. Hepatocytic maturation and differentiation of hFLPCs in liver organoids. (A) Immunostaining of liver organoids after 3 weeks of differentiation showing clusters of cells positively stained for mature hepatocyte markers such as ALB, HNF4 α , α 1-antitrypsin, and CYP3A4. Scale bar, 20 μ m. (B) RT-PCR analysis of glucose-6-phosphatase, aspartate aminotransferase, and tyrosine aminotransferase in liver organoids after 1 and 3 weeks of differentiation and in adult liver tissue. (C) Measurements of ALB and urea in conditioned media of liver organoids and hFLPCs in culture dishes during 3 weeks of differentiation (* $P < 0.05$). (D) RT-PCR analysis of the fetal isoform CYP3A4, adult isoform CYP3A7, CYP2B6, CYP2C9, and CYP2E1 in freshly isolated hFLPCs and liver organoids after 3 weeks of differentiation and in adult liver tissue. Abbreviations: A1AT, α 1-antitrypsin; AST, aspartate aminotransferase; DAPI, 4',6-diamidino-2-phenylindole; GAPDH, glyceraldehyde 3-phosphate dehydrogenase; G6PC, glucose-6-phosphatase; TAT, tyrosine aminotransferase.

(Fig. 2B); and the differentiated liver organoids also showed significantly higher ALB and urea secretion compared with hFLPCs differentiated in culture plates and Matrigel (Fig. 2C; Supporting Fig. S4). Due to the presence of a mixed population of cells within the discs including hepatocytes, the levels of ALB and urea are lower compared to 2D culture of adult hepatocytes (302 ng/mL/ng DNA and 1.25 mg/dL/ng DNA, respectively) when normalized using DNA content. To further evaluate the metabolic maturation of hFLPCs, gene expression analysis demonstrated increased expression of CYP3A4 at 3 weeks compared with 1 week of culture, whereas the expression of cytochrome P450 3A7 (CYP3A7) was slightly decreased after 3 weeks of culture (Fig. 2D). These isoforms represent postnatal and fetal isoforms of CYP450, respectively. In addition, different levels of expression of other CYP450 isoforms were confirmed by RT-PCR analysis, including CYP2B6, CYP2C9, and CYP2E1 (Fig. 2D). Finally, to demonstrate metabolic activity, we incubated the liver

organoids with diazepam and 7-ethoxy coumarin and detected the phase I metabolites temazepam (CYP3A4) and nordiazepam (CYP2C19/3A4), as well as 7-hydroxy coumarin (CYP2A6/2E1/1A2), respectively (Supporting Fig. S6 and S7). However, we failed to detect phase II glucuronic acid-conjugated metabolite. The liver organoids also expressed significantly higher levels of bile acid transporters expressed in hepatocytes such as bile salt export pump (BSEP) and sodium taurocholate cotransporting polypeptide (NTCP) compared to hFLPCs (Supporting Fig. S5), thus, further confirming progressive hepatic differentiation and maturation within the liver organoids.

BILE DUCT MORPHOGENESIS INSIDE THE SELF-ASSEMBLED LIVER ORGANIDS

The liver organoids exhibit different stages of bile duct morphogenesis including single or double ductal

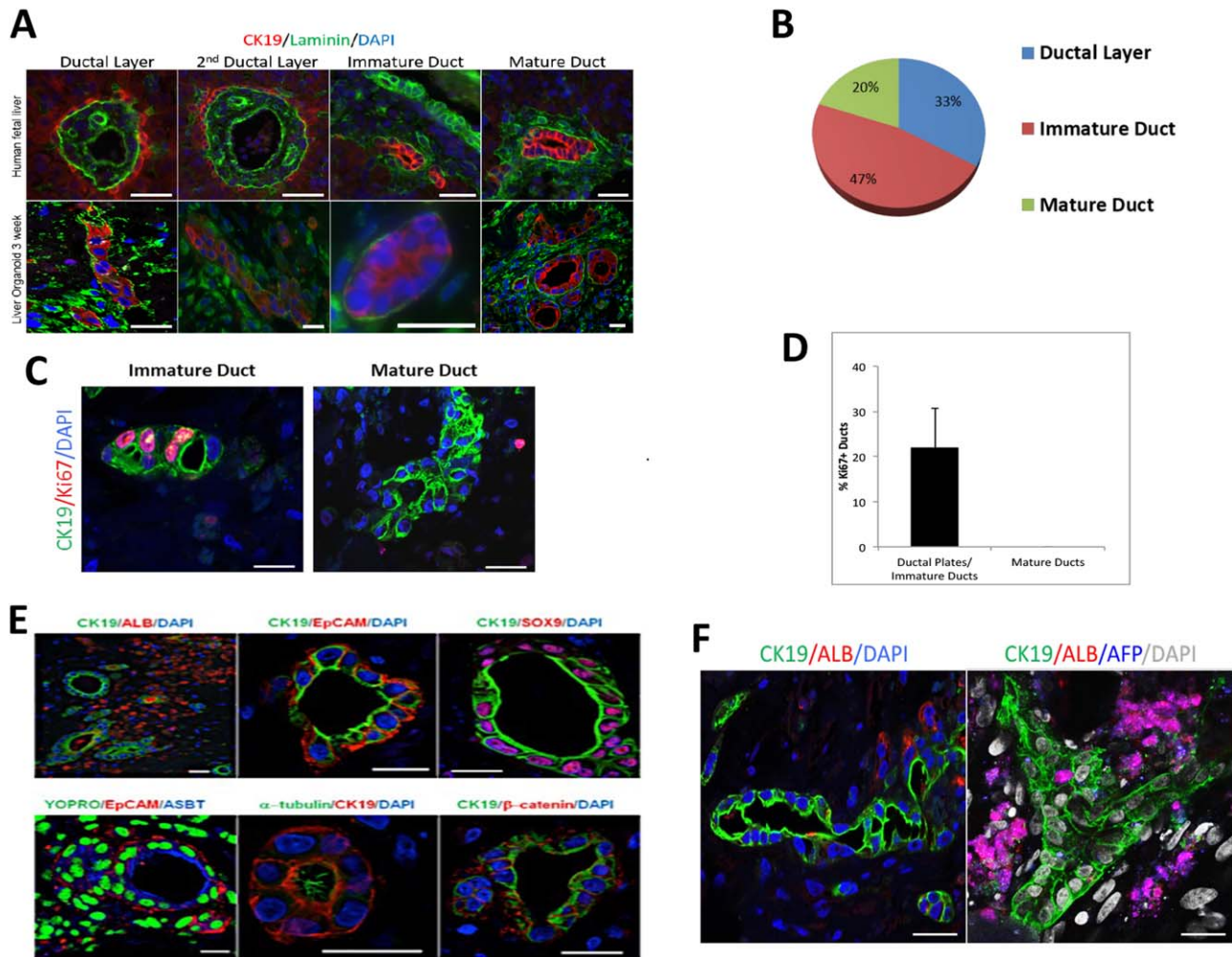


FIG. 3. Bile duct formation and cholangiocyte differentiation of hFLPCs in liver organoids. (A) Different stages of ductal morphogenesis in human fetal liver tissue (top panel) and liver organoids after 3 weeks of differentiation (bottom panel), stained with CK19 (red) or laminin (green; blue color denotes 4',6-diamidino-2-phenylindole–stained nuclei). (B) The relative proportions of the different stages of bile duct formations, as shown in (A), were quantified and are presented as percentages of total ductal structures. (C) Proliferating cells are observed in immature (left panel), but not in more mature ductal structures (right panel) (D) Graph representing percentage of Ki67–positive ducts in liver organoids. (E) Characterization of ductal structures formed in liver organoids after 3 weeks of differentiation using antibodies against CK19, ALB, EpCAM, acetylated α -tubulin, apical sodium–dependent bile transporter, β -catenin, and SOX9. (F) A bile duct structure of more than 100 μ m surrounded by ALB⁺ cells and branched biliary duct surrounded by AFP⁺/ALB⁺ hepatoblasts. Scale bar, 20 μ m. Abbreviations: ASBT, apical sodium–dependent bile transporter; DAPI, 4',6-diamidino-2-phenylindole.

layers, transient asymmetrical primitive ductal structures, immature ducts without defined lumen, and mature ductal structures, resembling duct developmental stages observed in human fetal liver (Fig. 3A). These stages were quantified as percentages of total biliary structures (CK19⁺/ALB⁻), showing 33% with single or double ductal layers, 47% immature ducts without defined lumen, and 20% mature ductal structures (Fig. 3B). Proliferating cells were observed in

some of the nascent immature ductal structures but were absent or detected only outside mature ducts, further indicating bile duct organogenesis in the liver organoids (Fig. 3C,D).

The ductal structures within the liver organoids were negative for albumin and positive for markers indicative of biliary tree progenitors and mature cholangiocytes including CK19, EpCAM, and SOX9 (Fig. 3E, top panels). Evidence that these ductal

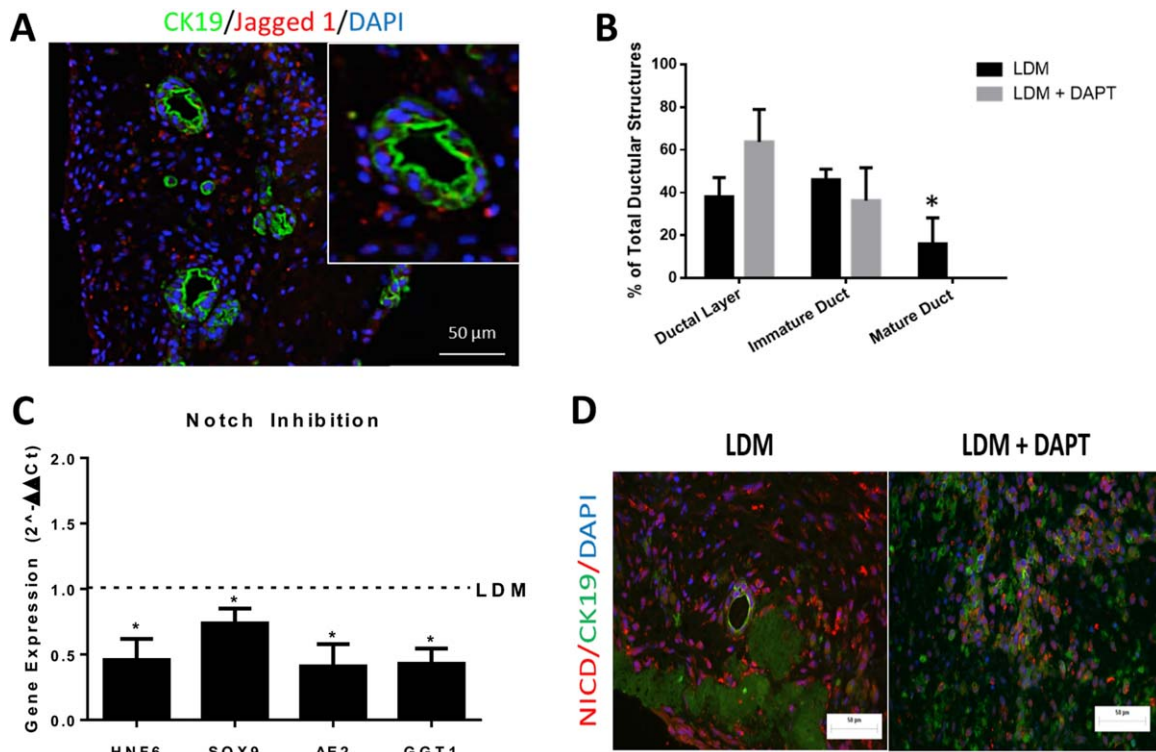


FIG. 4. Role of Jagged 1 in bile duct development. (A) Jagged 1 expression in cells surrounding CK19-positive bile duct structures inside the liver organoids after 3 weeks of differentiation (inset, higher magnification of a ductal structure). (B) hFLPCs, seeded in liver ECM discs, were differentiated for 3 weeks in LDM and LDM containing DAPT. The relative proportions of the different stages of bile duct formation were quantified and are presented as percentages of total ductal structures. (C) RT-PCR analysis of the expression of transcription factors regulating bile duct morphogenesis, HNF6 and SOX9, and of mature markers of cholangiocytes, anion exchange protein 2 and gamma-glutamyltransferase 1. (D) Notch intracellular domain (NICD) and CK19 expression in organoids treated with DAPT and control. * $P < 0.05$. Abbreviations: AE2, anion exchange protein 2; DAPI, 4',6-diamidino-2-phenylindole; GGT1, gamma-glutamyltransferase 1.

structures contain more mature cholangiocytes included (1) typical bile duct apical–basal polarity, (2) the presence of primary cilia (stained for α -acetylated tubulin) and apical sodium-dependent bile salt transporter in the apical membrane, and (3) β -catenin on the basolateral membrane (Fig 3E, bottom panels). Moreover, we observed long ductular structures with lumen spanning about several hundred micrometers (Fig. 3F) and a few branched ducts (Fig. 3F).

Signals from the portal mesenchyme, specifically Jagged 1, activate the Notch2 receptor and guide bile duct morphogenesis.^(20,21) The Notch ligand Jagged 1 is expressed in cells surrounding the ductal structures within the liver organoids (Fig. 4A). These cells were CK19-negative and ALB-negative, suggesting that they may represent the portal stellate cell population in the hFLPC preparation (Supporting Fig. S1). To further confirm the role of Notch signaling in bile duct

development in the liver organoids, we supplemented the LDM with an inhibitor of Notch signaling, DAPT. This inhibition increased the number of biliary structures at the earliest stage of ductal formation (ductal layer) and showed a trend toward a decrease in the number of immature ducts, with a total absence of mature ductal structures (Fig. 4B). In parallel, RT-PCR analysis showed a significant reduction in the expression of transcription factors regulating cholangiocyte differentiation including HNF6 and Sox9 and mature markers of cholangiocytes such as anion exchange protein 2 and gamma-glutamyltransferase 1 (Fig. 4C). To validate a reduction of Notch-2 signaling in our experimental setup, we performed a double immunofluorescence staining of Notch-2 notch intracellular domain and CK19 in the DAPT-inhibited and control liver organoids. The result was a visible decrease in Notch-2 notch intracellular domain

presence in the cells cultured in medium containing DAPT (Fig. 4D).

Discussion

In vitro models of human tissue and organ development mostly use human embryonic and induced pluripotent stem cells.^(22,23) However, these models do not fully recapitulate the simultaneous differentiation of liver progenitors to the hepatocytic and biliary fates and the formation of liver with these two tissues present. The generation of *bona fide* mature bile ducts is especially difficult *in vitro*^(21,24) and requires the presence of a 3D environment for efficient cellular polarization and organization.^(25,26) Scaffolds made from liver ECM were shown to possess the 3D environment that can guide differentiation and maturation of human liver progenitors.⁽²⁷⁾ Here, we demonstrate a model of self-assembled human liver organogenesis. Liver ECM discs were used as scaffolds for hFLPCs, resulting in 3D organoids that recapitulated to some extent the hepatobiliary differentiation of the fetal liver, including liver metabolic and secretory functions and formation of biliary tubular structures. We propose that the unique structure and composition of the liver ECM provide an environment for specific cell–ECM interactions that lead to the concomitant differentiation of hepatoblasts into hepatocytes and cholangiocytes. An important aspect of the current study was the use of a single culture media combination to achieve both hepatocytic and biliary differentiation of the hFLPCs. Others have used defined serum-free media, as well as specialized biomaterials, to differentiate human embryonic and induced pluripotent stem cells into functionally mature hepatocytes.^(28,29) Similarly, we compared Matrigel with our scaffold and showed that hFLPCs exposed to Matrigel in the same culture conditions did not completely mature into cholangiocytes and hepatocytes. Hence, these results clearly indicate that the liver ECM is superior in inducing maturation of hFLPCs into hepatocytes and biliary epithelium. Furthermore, we have documented the presence of laminin and collagen-IV around the developing bile duct structures and collagen-I and fibronectin in close proximity to the hepatocytes. Although we have not determined whether these molecules were already present in the acellular liver ECM preparations or secreted by the fetal cells, their presence at exact locations further strengthens our model. We have previously shown that hFLPCs cultured inside a ferret

liver ECM developed into a native liver tissue including hepatocytic and biliary structures,⁽¹³⁾ suggesting a conservation of cell differentiation signals from the ECM among different species. Additionally, double immunofluorescence staining of CK19/laminin, CK19/collagen-IV, ALB/fibronectin, and ALB/collagen-I suggested that the CK19⁺ or ALB⁺ cells were not the cells expressing those ECM molecules (Supporting Figs. S2D and S12). Hence, this provides a reliable indication that the fetal cells detected in these images synthesizing ECM molecules (collagen-I⁺, collagen-IV⁺, laminin⁺, or fibronectin⁺ cells) are most likely the stromal cell population present in the hFLPC preparations.

Models of tissue development have important applications in the discovery and treatment of human diseases. Especially in the liver, the Gunn rat model of inherited bilirubin–uridine diphosphate glucuronosyl transferase deficiency such as the Crigler-Najjar syndrome⁽³⁰⁾ and the *inv* mouse (partial deletion of the *inversin* gene) model of biliary atresia⁽³¹⁾ have been particularly helpful in the study of hepatic and biliary diseases, respectively. However, these models are not optimal for the study of human-specific congenital diseases and corresponding new therapeutic targets, due to differences in fetal liver development between species. Hepatocyte maturation is a dynamic process highlighted by changes in levels of various cytokines and transcription factors associated with differentiation and maturation of hepatoblasts into hepatocytes. The transcriptional switch from AFP to ALB is one of the hallmarks of hepatocyte maturation that was demonstrated in our liver organoid model. Unlike previously described bioengineered human liver tissue,⁽⁷⁾ our model also depicts a stepwise maturation process including inducible CYP450 isoforms. However, we were not able to document complete hepatocytic maturation because the organoids were not able to complete the metabolism of diazepam and 7-ethoxy coumarin beyond phase I metabolites. Additional immunofluorescence staining of hepatocytes and cholangiocytes present in adult and fetal liver sections with mature markers previously used in our liver organoid analysis (Figs. 2 and 3) presented a phenotype for these cells more comparable to fetal/neonatal bile ducts and hepatocytes rather than adult. Expression of some adult markers was similar to the adult liver (HNF4 α , ALB, CYP3A4, CK19, etc.). However, some were equally absent in fetal liver sections and in our organoids (Aquaporin-4, anion exchange protein 2, etc.) (Supporting Figs. S8–S10). These suggest that the

differentiated cells within the organoids present an immature phenotype, which we believe could be potentially further matured in culture.

Models depicting development of the bile ductal structures are also important to study hereditary biliary atresia diseases. The liver organoids showed a progressive trend of developmental generation of bile duct structures by histology, but molecular analysis (RT-PCR) did not show a progressive increase in mature cholangiocyte markers. As mentioned above, we believe that this was probably due to a cellular phenotype more similar to a fetal/neonatal bile duct rather than that of an adult. In Alagille syndrome, for example, mutations in Jagged 1 lead to inactive Notch pathway, causing bile duct paucity or biliary atresia.^(32,33) During fetal development, signals from adjacent cells, such as endothelial and stellate cells, regulate bile duct organization around the portal mesenchyme.^(20,34-36) Flow-cytometric (fluorescence-activated cell sorting) analysis showed that hFLPC preparations contain a population of stromal and endothelial cells (Supporting Fig. S1) that can be found surrounding hepatocyte clusters and biliary structures in liver organoids cultured for 3 weeks (Supporting Fig. S11). Furthermore, this stromal population (alpha-smooth muscle active-positive) found in hFLPC preparations most probably contains the cells expressing the Notch ligand Jagged 1 that supported bile duct development and maturation in the liver organoids.⁽²⁰⁾ To validate the role of Notch signaling in bile duct development in the liver organoids, a Notch inhibitor, DAPT, which inhibits γ -secretase, was added to the liver differentiation culture media. We observed attenuated maturation of the bile duct structures along with significant reduction in the expression of transcription factors regulating bile duct development.

Besides providing a better model for human liver development, the liver organoids may be used for drug development and toxicity screening applications. New drugs are usually tested in rodent models for predicted toxicity; however, rodent metabolism is different from that in humans. Cultures of human hepatocytes have been developed to address this limitation. The self-assembled organoids present significantly more complex liver structures compared with 2D *in vitro* hepatocyte culture and simple 3D gel-based hepatocyte culture systems and, thus, have a higher potential to accurately predict drug metabolism and toxicity. The current study presents self-assembled liver organoids consisting of hepatocytes and biliary structures. The liver organoids replicate some of the key processes of

fetal liver development, which can be manipulated *in vitro* to hinder bile duct development, creating a model exhibiting a phenotype similar to Alagille syndrome. These results are similar in many aspects to previous data from other *in vitro* models using differentiated cholangiocytes from pluripotent stem cells.^(3,37,38) However, none of these previous studies presented long or branched biliary ducts or the step-by-step developmental stages of bile duct organogenesis. Furthermore, our model has the potential to become an *in vitro* system to test drug teratogenesis in the liver, including a novel class of drugs targeting the Notch pathway (γ -secretase inhibitors) that are under clinical trials for multiple diseases.⁽³⁹⁾ Nonetheless, future efforts should address the lack of fully developed non-parenchymal components, such as the vasculature and mesenchyme, as well as the presence of cells from the innate immune system (Kupffer cells), with important roles in the inflammation cascade. Collectively, the liver organoids developed here can serve as a tool to study congenital diseases, develop novel therapeutic strategies, and provide important information to guide research toward creating functional tissues for transplantation in patients suffering from end-stage diseases.

Acknowledgment: Lola Reid, Ph.D., made suggestions for improvements in the experiments and in the manuscript, and Dr. Eliane Wauthier assisted in the preparation of media and of cells.

REFERENCES

- 1) Godoy P, Hewitt NJ, Albrecht U, Andersen ME, Ansari N, Bhattacharya S, et al. Recent advances in 2D and 3D *in vitro* systems using primary hepatocytes, alternative hepatocyte sources and non-parenchymal liver cells and their use in investigating mechanisms of hepatotoxicity, cell signaling and ADME. *Arch Toxicol* 2013;87:1315-1530.
- 2) Sampaziotis F, Cardoso de Brito M, Madrigal P, Bertero A, Saeb-Parsy K, Soares FA, et al. Cholangiocytes derived from human induced pluripotent stem cells for disease modeling and drug validation. *Nat Biotechnol* 2015;33:845-852.
- 3) Ogawa M, Ogawa S, Bear CE, Ahmadi S, Chin S, Li B, et al. Directed differentiation of cholangiocytes from human pluripotent stem cells. *Nat Biotechnol* 2015;33:853-861.
- 4) Khetani SR, Bhatia SN. Microscale culture of human liver cells for drug development. *Nat Biotechnol* 2008;26:120-126.
- 5) Drewitz M, Helbling M, Fried N, Bieri M, Moritz W, Lichtenberg J, et al. Towards automated production and drug sensitivity testing using scaffold-free spherical tumor microtissues. *Biotechnol J* 2011;6:1488-1496.

- 6) Katsuda T, Kojima N, Ochiya T, Sakai Y. Biliary epithelial cells play an essential role in the reconstruction of hepatic tissue with a functional bile ductular network. *Tissue Eng Part A* 2013;19:2402-2411.
- 7) Takebe T, Sekine K, Enomura M, Koike H, Kimura M, Ogari T, et al. Vascularized and functional human liver from an iPSC-derived organ bud transplant. *Nature* 2013;499:481-484.
- 8) Huch M, Gehart H, van Boxtel R, Hamer K, Blokzijl F, Verstegen MM, et al. Long-term culture of genome-stable bipotent stem cells from adult human liver. *Cell* 2015;160:299-312.
- 9) Tateno C, Yoshizane Y, Saito N, Kataoka M, Utoh R, Yamasaki C, et al. Near completely humanized liver in mice shows human-type metabolic responses to drugs. *Am J Pathol* 2004;165:901-912.
- 10) Azuma H, Paulk N, Ranade A, Dorrell C, Al-Dhalimy M, Ellis E, et al. Robust expansion of human hepatocytes in *Fah^{-/-}/Rag2^{-/-}/Il2rg^{-/-}* mice. *Nat Biotechnol* 2007;25:903-910.
- 11) Chen AA, Thomas DK, Ong LL, Schwartz RE, Golub TR, Bhatia SN. Humanized mice with ectopic artificial liver tissues. *Proc Natl Acad Sci USA* 2011;108:11842-11847.
- 12) **Seok J, Warren HS, Cuenca AG, Mindrinos MN, Baker HV, Xu W, et al.** Genomic responses in mouse models poorly mimic human inflammatory diseases. *Proc Natl Acad Sci USA* 2013;110:3507-3512.
- 13) **Baptista PM, Siddiqui MM, Lozier G, Rodriguez SR, Atala A, Soker S.** The use of whole organ decellularization for the generation of a vascularized liver organoid. *HEPATOLOGY* 2011;53:604-617.
- 14) Baptista PM, Vyas D, Moran E, Wang Z, Soker S. Human liver bioengineering using a whole liver decellularized bioscaffold. *Methods Mol Biol* 2013;1001:289-298.
- 15) Kubota H, Reid LM. Clonogenic hepatoblasts, common precursors for hepatocytic and biliary lineages, are lacking classical major histocompatibility complex class I antigen. *Proc Natl Acad Sci USA* 2000;97:12132-12137.
- 16) Baptista PM, Orlando G, Mirmalek-Sani SH, Siddiqui M, Atala A, Soker S. Whole organ decellularization—a tool for bioscaffold fabrication and organ bioengineering. *Conf Proc IEEE Eng Med Biol Soc* 2009;2009:6526-6529.
- 17) **Baptista PM, Moran EC, Vyas D, Ribeiro MH, Atala A, Sparks JL, et al.** Fluid flow regulation of revascularization and cellular organization in a bioengineered liver platform. *Tissue Eng Part C Methods* 2016;22:199-207.
- 18) **Antoniou A, Raynaud P, Cordi S, Zong Y, Tronche F, Stanger BZ, et al.** Intrahepatic bile ducts develop according to a new mode of tubulogenesis regulated by the transcription factor SOX9. *Gastroenterology* 2009;136:2325-2333.
- 19) Maher JJ, Bissell DM. Cell–matrix interactions in liver. *Semin Cell Biol* 1993;4:189-201.
- 20) Hofmann JJ, Zovein AC, Koh H, Radtke F, Weinmaster G, Iruela-Arispe ML. *Jagged1* in the portal vein mesenchyme regulates intrahepatic bile duct development: insights into Alagille syndrome. *Development* 2010;137:4061-4072.
- 21) Si-Tayeb K, Lemaigre FP, Duncan SA. Organogenesis and development of the liver. *Dev Cell* 2010;18:175-189.
- 22) Lancaster MA, Knoblich JA. Organogenesis in a dish: modeling development and disease using organoid technologies. *Science* 2014;345:1247-1252.
- 23) Medvinsky A, Livesey FJ. On human development: lessons from stem cell systems. *Development* 2015;142:17-20.
- 24) Navarro-Alvarez N, Soto-Gutierrez A, Kobayashi N. Hepatic stem cells and liver development. *Methods Mol Biol* 2010;640:181-236.
- 25) Ader M, Tanaka EM. Modeling human development in 3D culture. *Curr Opin Cell Biol* 2014;31:23-28.
- 26) Chistiakov DA. Liver regenerative medicine: advances and challenges. *Cells Tissues Organs* 2012;196:291-312.
- 27) Wang Y, Cui CB, Yamauchi M, Miguez P, Roach M, Malavarca R, et al. Lineage restriction of human hepatic stem cells to mature fates is made efficient by tissue-specific biomatrix scaffolds. *HEPATOLOGY* 2011;53:293-305.
- 28) Medine CN, Lucendo-Villarin B, Storck C, Wang F, Szkolnicka D, Khan F, et al. Developing high-fidelity hepatotoxicity models from pluripotent stem cells. *Stem Cells Transl Med* 2013;2:505-509.
- 29) Villarin BL, Cameron K, Szkolnicka D, Rashidi H, Bates N, Kimber SJ, et al. Polymer supported directed differentiation reveals a unique gene signature predicting stable hepatocyte performance. *Adv Healthc Mater* 2015;4:1820-1825.
- 30) Gunn CK. Hereditary acholuric jaundice in the rat. *Can Med Assoc J* 1944;50:230-237.
- 31) Mazziotti MV, Willis LK, Heuckeroth RO, LaRegina MC, Swanson PE, Overbeek PA, et al. Anomalous development of the hepatobiliary system in the *Inv* mouse. *HEPATOLOGY* 1999;30:372-378.
- 32) McCright B, Lozier J, Gridley T. A mouse model of Alagille syndrome: *Notch2* as a genetic modifier of *Jag1* haploinsufficiency. *Development* 2002;129:1075-1082.
- 33) Geisler F, Nagl F, Mazur PK, Lee M, Zimmer-Strobl U, Strobl LJ, et al. Liver-specific inactivation of *Notch2*, but not *Notch1*, compromises intrahepatic bile duct development in mice. *HEPATOLOGY* 2008;48:607-616.
- 34) Raynaud P, Carpentier R, Antoniou A, Lemaigre FP. Biliary differentiation and bile duct morphogenesis in development and disease. *Int J Biochem Cell Biol* 2011;43:245-256.
- 35) Zong Y, Stanger BZ. Molecular mechanisms of bile duct development. *Int J Biochem Cell Biol* 2011;43:257-264.
- 36) **Fabris L, Cadamuro M, Libbrecht L, Raynaud P, Spirli C, Fiorotto R, et al.** Epithelial expression of angiogenic growth factors modulate arterial vasculogenesis in human liver development. *HEPATOLOGY* 2008;47:719-728.
- 37) Sampaziotis F, Cardoso de Brito M, Madrigal P, Bertero A, Saeb-Parsy K, Soares FA, et al. Cholangiocytes derived from human induced pluripotent stem cells for disease modeling and drug validation. *Nat Biotechnol* 2015;33:845-852.
- 38) Kamiya A, Chikada H. Human pluripotent stem cell-derived cholangiocytes: current status and future applications. *Curr Opin Gastroenterol* 2015;31:233-238.
- 39) Andersson ER, Lendahl U. Therapeutic modulation of Notch signalling—are we there yet? *Nat Rev Drug Discov* 2014;13:357-378.

Author names in bold designate shared co-first authorship.

Supporting Information

Additional Supporting Information may be found at onlinelibrary.wiley.com/doi/10.1002/hep.29483/supinfo.